Journal of Molecular Structure 1006 (2011) 259–265

Contents lists available at SciVerse ScienceDirect

Journal of Molecular Structure

journal homepage: www.elsevier.com/locate/molstruc

Novel substituted 1-iminoisoindoline derivatives: Synthesis, structure determination and antiproliferative activity

Irena Sović [a], Vladimir Stilinović [b], Branko Kaitner [b], Sandra Kraljević-Pavelić [c,1], Maro Bujak [c], Katarina Čuljak [b], Predrag Novak [b], Grace Karminski-Zamola [a,*]

[a] Department of Organic Chemistry, Faculty of Chemical Engineering and Technology, University of Zagreb, Marulićev trg 20, P.O. Box 177, HR-10000 Zagreb, Croatia
[b] Department of Chemistry, Faculty of Science, University of Zagreb, Horvatovac 102a, HR-10000 Zagreb, Croatia
[c] Laboratory for Systemic Biomedicine, Division of Molecular Medicine, Ruđer Bošković Institute, Bijenička 54, 10000 Zagreb, Croatia

ARTICLE INFO

Article history:
Received 27 June 2011
Received in revised form 6 September 2011
Accepted 6 September 2011
Available online 16 September 2011

Keywords:
1-Iminoisoindoline derivatives
Synthesis
Structure determination
Spectroscopic characterization
Thermal analysis
Antiproliferative activity

ABSTRACT

Novel derivatives of isoindoline, *N*-phenyl-1-iminophenylisoindoline **6**, *N*-(4-methylphenyl)-1-imino-(4-methylphenyl)-isoindoline **7**, *N*-(pyridin-2-yl)-1-imino-(pyridin-2-yl)-isoindoline **8** and *N*-(5-methylpyridin-2-yl)-1-imino(5-methylpyridin-2-yl)-isoindoline **9** were prepared by the reaction of condensation of phthalaldehyde and corresponding amines. Structures of all compounds have been studied using one- and two-dimensional ^{1}H and ^{13}C NMR, IR, MS and UV/Vis spectroscopy. The crystal and molecular structures of **7**, **8** and **9** were determined by X-ray diffraction on single crystals. In all three molecules the isoindoline system and its *N*-substituent are approximately coplanar. The crystal structures comprise of discrete molecules linked only by weak C–H···N interactions in the case of **8** and **9**. NMR analysis showed that conformations of compounds **6** and **7** differ from those of **8** and **9** in solution. Differences between solution and solid state structures were also noticed. All prepared compounds were tested on their antiproliferative activity *in vitro*. Compound **7** exerted the strongest non-specific antiproliferative effect on all cell lines and compounds **8** and **9** showed selective antiproliferative effect on HepG2 cell line.

© 2011 Elsevier B.V. All rights reserved.

1. Introduction

Isoindoline and its derivatives have in recent years attracted a great attention from medicinal and synthetic organic chemists due to their wide range of biological activities as well as their application in herbicide and dye industries. They are present in many natural and synthetic biologically active compounds which have been reported to possess psychostimulant, analgesic, antiinflammatory, antifungal, antipyretic and antitumor properties [1–6]. For example, staurosporine isolated from bacteria *Streptomices staurosporeus* acts as a protein kinase C inhibitor; indoprofen, a synthetic derivative of isoindoline, is an anti-inflammatory drug; pazinaclone is an anxiolytic agent; *N*-substituted derivatives inhibit dipeptidyl peptidases 8 and 9 which are active in Type II diabetes [7–9]. Isoindoline derivatives are useful intermediates in organic synthetic chemistry as precursors for the synthesis of various important drugs and natural products [10]. More recently complexes of isoindoline derivatives with biological activity have been reported [11,12]. Derivatives of isoindoline are also very effective plant growth regulating agents [13]. Also several patents on dyes and pigments involving isoindoline based structures for colouring high molecular weight organic materials have been granted [14,15]. They also have an application as ligands in coordination and organometallic chemistry [16–19] since they form complexes that are excellent precatalysts for CC coupling reactions, aldol condensations and other transformations.

The scope of this study was to synthesize some novel aryl and heteroaryl substituted 1-iminoisoindolines, determine their crystal structure and screen their antiproliferative effects on human tumor cell lines in comparison with their structure. For the isoindoline synthesis a number of different methods are available, depending on the starting material [20–23]. When phthalaldehyde is used as a starting material, products of the reaction are highly dependant on the reaction conditions [24–27]. Here we used condensation of phthalaldehyde and amines in mild neutral conditions.

2. Experimental section

2.1. Synthesis

2.1.1. Instrumental methods of detection

Melting points were determined on a Mettler Toledo TGA/SDTA 851 and DSC823 modules. IR spectra were recorded on a Bruker

* Corresponding author. Tel.: +385 1 4597 215; fax: +385 1 4597 224.
E-mail address: gzamola@fkit.hr (G. Karminski-Zamola).
[1] Present address: Department of Biotechnology, University of Rijeka, Trg braće Mažuranića 10, HR-51000 Rijeka, Croatia.

0022-2860/$ - see front matter © 2011 Elsevier B.V. All rights reserved.
doi:10.1016/j.molstruc.2011.09.017

Vertex 70 spectrophotometer with diamond crystal. Mass spectra were recorded on an Agilent 1200 series LC/6410 QQQ instrument. Elemental analysis for carbon, hydrogen and nitrogen were performed on a Perkin-Elmer, Series II, CHNS Analyzer 2400. Where analyses are indicated only as symbols of elements, analytical results obtained are within 0.4% of the theoretical value. All compounds were routinely checked by thin layer chromatography (TLC) using precoated *Merck* silica gel 60F-254 plates and the spots were detected under UV light (254 nm).

2.1.2. General procedure of preparation

A mixture of phthalaldehyde and a corresponding amine in absolute ethanol was stirred at room temperature for 1.5–48 h. The resulting product was then filtered off and recrystallized from ethanol or ethanol/dichlormethane to obtain powder or crystals.

*2.1.3. N-phenyl-1-iminophenylisoindoline **6***

Compound **6** was prepared using the general method described for the preparation of compounds **6**–**9**; a mixture of phthalaldehyde **1** (0.54 g, 4 mmol) and aniline **2** (0.73 ml, 8 mmol) in absolute ethanol (15 ml) was stirred at room temperature for 1.5 h. The obtained precipitate was filtered off and recrystallized from ethanol/dichloromethane to give 0.86 g (76%) of yellow powder; mp = 128 °C, decomposition (mp_{lit} = 128–129.5 °C)[28].

*2.1.4. N-(4-methylphenyl)-1-imino-(4-methylphenyl)-isoindoline **7***

Compound **7** was prepared from a mixture of phthalaldehyde **1** (0.67 g, 5 mmol) and 4-methylaniline **3** (1.07 g, 10 mmol) in absolute ethanol (20 ml) by stirring at room temperature for 2 h. The yield of yellow crystals after repeated recrystallisation was 0.69 g (44%); mp = 115 °C, decomposition; IR (diamond) (ν/cm^{-1}): 3050, 1649, 1585; MS (*m/z*): 313.3 ([M + 1]$^+$); Anal. Calcd. for $C_{22}H_{20}N_2$: C, 84.58; H, 6.45; N, 8.97. Found: C, 84.86; H, 6.47; N, 8.95.

*2.1.5. N-(pyridin-2-yl)-1-imino-(pyridin-2-yl)-isoindoline **8***

Compound **8** was prepared from a mixture of phthalaldehyde **1** (0.67 g, 5 mmol) and 2-aminopyridine **4** (0.94 g, 10 mmol) in absolute ethanol (20 ml) after 24 h stirring. The yield of orange crystals after recrystallization from ethanol was 0.83 g (58%); mp 203.6 °C; IR (diamond) (ν/cm^{-1}): 3048, 1643, 1581; MS (*m/z*): 287.2 ([M + 1]$^+$); Anal. Calcd. for $C_{18}H_{14}N_4$: C, 75.50; H, 4.93; N, 19.57. Found: C, 75.27; H, 4.95; N, 19.52.

*2.1.6. N-(5-methylpyridin-2-yl)-1-imino-(5-methylpyridin-2-yl)-isoindoline **9***

Compound **9** was prepared from a mixture of phthalaldehyde **1** (0.54 g, 4 mmol) and 2-amino-5-methylpyridine **5** (0.86 g, 8 mmol) in absolute ethanol (20 ml) after 48 h stirring. The yield of yellow crystals after repeated recrystallization from ethanol was 0.45 g (36%); mp 187.6 °C; IR (diamond) (ν/cm^{-1}): 3082, 1647, 1548; MS (*m/z*): 315.3 ([M + 1]$^+$); Anal. Calcd. for $C_{20}H_{18}N_4$: C, 76.41; H, 5.77; N, 17.82. Found: C, 76.65; H, 5.74; N, 17.87.

2.2. X-ray structure determination

The crystal and molecular structures of **7**, **8** and **9** were determined by single crystal X-ray diffraction, while **6** formed very thin crystals unsuitable for diffraction experiments. The diffraction data were collected at 295 K for all three crystals. Diffraction measurements were made on an Oxford Diffraction Xcalibur Kappa CCD X-ray diffractometer with graphite-monochromated Mo Kα (λ = 0.71073 Å) radiation [29]. The data sets were collected using the ω scan mode over the 2θ range up to 54°. The structures were solved by the direct methods and refined using SHELXS and SHELXL programs [30]. The structural refinement was performed on F^2 using all data. The hydrogen atoms were placed in calculated positions and treated as riding on their parent atoms [C–H = 0.93 Å and U_{iso}(H) = 1.2 U_{eq}(C); C–H = 0.97 Å and U_{iso}(H) = 1.2 U_{eq}(C)]. All calculations were performed and the drawings were prepared using WINGX crystallographic suite of programs [31]. The crystal data are listed in Table 1. Further details are available from the Cambridge Crystallographic Center with quotation numbers 799224–799226.

2.3. NMR measurements

One- and two-dimensional (^{1}H, APT, gCOSY, gHSQC and gHMBC) NMR spectra were recorded at ambient temperature on Varian Gemini 300 and Bruker Avance DPX300 spectrometers using a 5 mm diameter inverse detection probe with *z*-gradient accessory. The spectra were recorded in DMSO-d_6 with the sample concentration of 20 mg ml^{-1} and TMS as the internal standard.

The typical spectral conditions for one-dimensional ^{1}H and ^{13}C (APT) spectra were as follows. The spectra were recorded using 64 K data points and spectral widths of 6200 Hz and 20000 Hz for proton and carbon (APT) experiments, respectively. Digital resolution was 0.10 Hz and 0.30 Hz per point, respectively. The number of scans was 8–16 for ^{1}H and 1000–3000 for APT spectra.

Two-dimensional gCOSY and NOESYspectra were recorded under the following conditions: spectral width was 6000 Hz in both dimensions, 2 K data points were applied in time domain and 512 increments were collected for each data set with linear prediction to 1 K and zero filling to 2 K. The number of scans per increment varied between 4 and 32. A relaxation delay was 1.5 s. States-TPPI NOESY spectra were obtained with the mixing time of 400 ms and processed with sine squared function shifted by $\pi/2$ in both domains, while gsCOSY spectra were processed with unshifted sine function. The digital resolution was 2.7 and 10.7 Hz per point in f2 and f1 domains, respectively.

The gradient selected inverse ^{1}H–^{13}C correlation experiments, gHSQC and gHMBC were recorded using the acquisition matrix of 1 K × 256 with 32 scans and processed with 2 K × 1 K transformed matrix. The sweep width was 7500 Hz in f2 dimension and 31500 Hz in f1 dimension for both experiments. Spectra were

Table 1
Crystallographic data for compounds **7**, **8** and **9**.

	7	**8**	**9**
Formula	$C_{22}H_{20}N_2$	$C_{18}H_{14}N_4$	$C_{20}H_{18}N_4$
M_r	312.4	286.33	314.38
T (K)	295(2)	295(2)	295(2)
Crystal system	Orthorhombic	Triclinic	Triclinic
Space group	*P nma*	$P\bar{1}$	$P\bar{1}$
a (Å)	19.0183(9)	8.256(3)	7.5688(11)
b (Å)	7.1748(4)	8.276(3)	9.0096(11)
c (Å)	12.7725(5)	12.525(4)	12.9767(15)
α (°)	90	105.87(3)	81.338(10)
β (°)	90	92.34(3)	87.048(10)
γ (°)	90	118.45(4)	68.892(12)
V (Å^3)	1742.84(14)	708.8(6)	816.11(18)
Z	4	2	2
ρ_{calc} (g cm^{-3})	1.191	1.342	1.279
Radiation	Mo Kα	Mo Kα	Mo Kα
μ (mm^{-1})	0.07	0.083	0.078
h, k, l range	$-24 < h < 23$	$-8 < h < 10$	$-9 < h < 9$
	$-9 < k < 8$	$-10 < k < 10$	$-11 < k < 11$
	$-16 < l < 16$	$-15 < l < 15$	$-16 < l < 12$
Reflections collected	12,368	8362	7175
Reflections unique	2049	3081	3497
Reflections observed ($I > 2\sigma(I)$)	1371	2314	3088
R_1(obs)	0.0729	0.0686	0.0496
wR_2(obs)	0.1549	0.1521	0.1391
GooF	1.112	1.106	1.072

processed with a shifted sine bell window function and linear prediction. Digital resolution was 3.25 Hz per point and 30.70 Hz per point in f2 and f1, respectively. HMBC spectra were recorded using transfer delay for the evolution of long range C–H couplings of 60 ms.

2.4. Thermal and spectroscopic analysis

Thermal analysis was carried out on a Mettler Toledo TGA/SDTA 851 and DSC823 modules in sealed aluminum pans (40 μL), heated in flowing nitrogen (200 mL min^{-1}) at 7 °C min^{-1}. The data collection and analysis was performed by program package *STAR*[e] *Software 9.01* [32].

The electronic absorption spectra were recorded on a Varian Cary 100 spectrophotometer using quartz cuvettes (1 cm), in ethanol at the concentration of 2.0×10^{-5} mol dm^{-3}.

3. Results and discussion

3.1. General aspects of preparation

N-phenyl-1-iminophenylisoindoline **6**, *N*-(4-methylphenyl)-1-imino-(4-methylphenyl)-isoindoline **7**, *N*-(pyridin-2-yl)-1-imino-(pyridin-2-yl)-isoindoline **8** and *N*-(5-methylpyridin-2-yl)-1-imino(5-methylpyridin-2-yl)-isoindoline **9** were prepared according to the Scheme 1 in the reaction of condensation of phthalaldehyde and different amines: aniline, 4-methylaniline, 2-aminopyridine and 2-amino-5-methylpyridine respectively in absolute ethanol at room temperature. *N*-phenyl-1-iminophenylisoindoline **6** had already been described in the literature [28], but in this work different reaction conditions were used and in that way the reaction time is shortened from 12 h to 1.5 h with similar yield. There are also reported attempts of the condensation using amines possessing the heteroatom (nitrogen, sulfur) at the 2-position but the isolated product was 1,3-dihydroxyisoindoline [33]. Solely by changing the solvent from diethyl ether to ethanol we obtained the desired products **8** and **9** which indicates that polar protic solvents are likely to have influence on the formation of iminoisoindoline. These findings are in agreement with high dependence on the reaction conditions of this type of reaction.

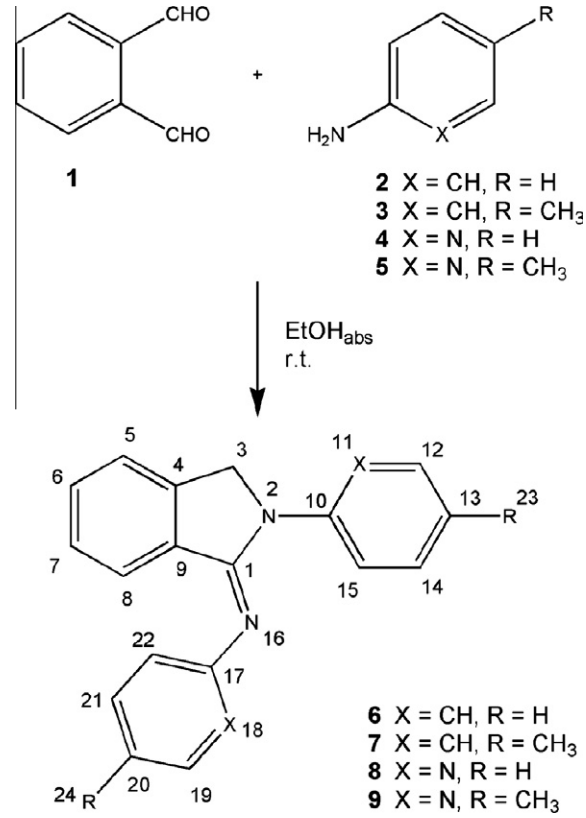

Scheme 1. Reaction scheme for preparation of isoindoline derivatives **6**–**9**.

3.2. X-ray structure determination

Compound **7** (Fig. 1.) crystallizes in the orthorhombic *P nma* space group with four molecules per unit cell. The small size and weak diffraction of the measured crystals rendered the final *R* factor somewhat higher than expected for small molecules (0.073), however this does not have a significant effect on the structural model precision. The molecule is tetracyclic with two 4-methylphenyl groups bonded to the isoindoline system. The phenyl ring bonded to the isoindoline nitrogen is coplanar with the isoindoline system, as well as the imino group. The phenyl ring bonded to the imino group is at a right angle to the rest of the molecule. This renders the molecular symmetry *Cs* and the molecules are placed on crystallographic mirror planes. The molecular geometry is stabilized by an intermolecular C14–H14···N2 contact of 2.872 Å between the imino nitrogen atom and an *ortho*-carbon of the 4-methylphenyl bonded to the isoindoline nitrogen. There are no significant intermolecular bonds as the molecules are stacked by π–π contacts along the *b* axis.

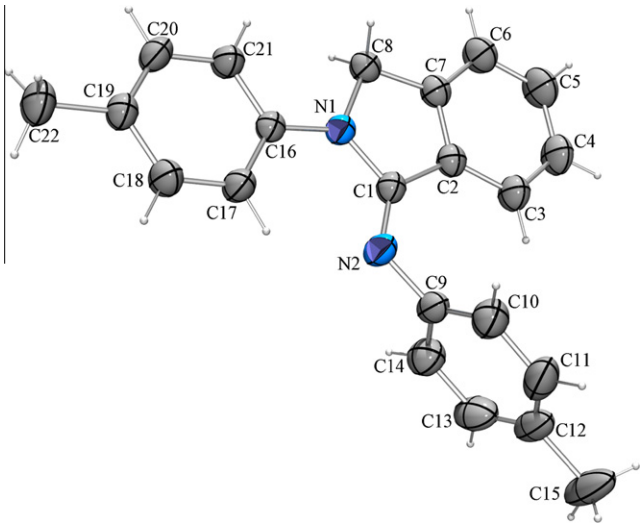

Fig. 1. Molecular structure of **7** with the atom labeling scheme. Thermal ellipsoids are drawn at the 50% probability level and hydrogen atoms are presented as spheres of arbitrary small radii.

The structure of compound **8** (Fig. 2.) corresponds to that published in the literature [34]. The pyridine ring bonded to the isoindoline system is at a dihedral angle of only *ca.* 7.6° and the pyridine ring bonded to the imino group is at a dihedral angle of *ca.* 79.1° to the isoindoline system. The molecular geometry is stabilized by an intramolecular C15–H15···N2 contact of 2.888 Å between the imino nitrogen atom and the *ortho*-carbon of the 2-pyridyl bonded to the isoindoline nitrogen. The molecules are interconnected by C6–H6···N4 (forming an R_2^2 (14) hydrogen bonding motif) and C13–H13···N3 (forming an R_2^2 (8) hydrogen bonding motif) hydrogen bonds over inversion centers into chains along the [−1 0 1] direction. The chains are further interconnected by C5–H5···N3 hydrogen bonds into sheets perpendicular to the *b* axis (Fig. 3a.). The geometric parameters of intermolecular C–H···N contacts for

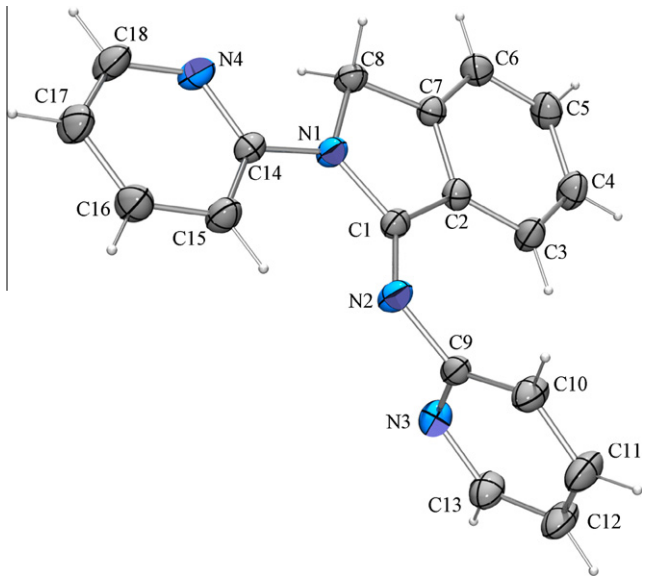

Fig. 2. Molecular structure of **8** with the atom labeling scheme. Thermal ellipsoids are drawn at the 50% probability level and hydrogen atoms are presented as spheres of arbitrary small radii.

compounds **8** and **9** are given in Table 2.Compound **9** (Fig. 4.) crystallizes in the triclinic $P\,\bar{1}$ space group with two molecules per unit cell. The 4-methyl-2-pyridine cyclic group bonded to the isoindoline system is almost coplanar with it, with a dihedral angle of only *ca.* 4.1°. The 4-methyl-2-pyridine group bonded to the imino group is at a dihedral angle of *ca.* 69.6° to the isoindoline system. The molecular geometry is stabilized by an intramolecular C16–H16···N2 contact of 2.860 Å between the imino nitrogen atom and the *ortho*-carbon of the 4-methyl-2-pyridyl group bonded to the isoindoline nitrogen. The molecules are interconnected by C10–H10···N4 (forming an R_2^2 (16) hydrogen bonding motif) and C13–H13···N3 (forming an R_2^2 (8) hydrogen bonding motif) hydrogen bonds over inversion centers into chains along the [0 − 1 1] direction. The chains are further interconnected by C5–H5···N3 hydrogen bonds into sheets perpendicular to the *a* axis (Fig. 3b).

Molecular geometries of all three compounds are quite similar, differing slightly only by rotation of the ring bonded to the imino group (Fig. 5.). They are also similar to the molecular structures of previously reported 1-imino isoindoline derivatives [35,36] as well as corresponding cations with protonated imino nitrogen [37]. Calculation of packing densities for the three compounds yielded packing coefficients of 66.7 for **7**, 69.6 for **8** and 68.2 for **9**. The higher packing efficiency (as well as density; Table 1.) for **8** and **9** in comparison to **7**, may be attributed to the existence of intermolecular C–H···N hydrogen bonds which are present the structures of **8** and **9**, but not in the structure of **7**, in which lacks suitable hydrogen acceptors.

3.3. Thermal analysis

Melting points, enthalpies and entropies for compounds **8** and **9** are given in Table 3. The melting point of **8** is 16.0 °C higher than that of **9**, which can probably be attributed to stronger (*i. e.* shorter) C–H···N hydrogen bonds which interconnect molecules in its crystal structure [38]. Although at the first glance enthalpies of fusion might seem to contradict this conclusion, the melting enthalpy of **9** being 5.3 kJ mol^{-1} higher then that for **8**, it should be remembered that the enthalpy of fusion is dependant on enthalpies of formation of both the solid and the melt, and therefore cannot be used as a measure of lattice energy.

Compound **7** upon heating irreversibly decomposes. The decomposition initiates at approximately 115 °C and is marked in the DSC curve by a strong exothermic signal followed immediately by a somewhat weaker endothermic signal. The overall enthalpy change is −6.9 kJ mol^{-1}, rendering the decomposition exothermic. There is only a minor change of the sample mass which accompanies this process since the mass reduces by 0.21% (Fig. 6.). Similar behavior is noticed in compound **6**, where an exothermic signal appears at 128 °C and is also immediately followed by an endothermic signal. The overall enthalpy change is −19.64 kJ mol^{-1}, rendering the decomposition even more exothermic than that of **7**. It should be emphasized that no such thermal behavior is noticed in compounds **8** and **9.** It appears therefore that the presence of nitrogen in the *o*-position in pyridine derivatives **8** and **9** has an important effect on the thermal stability of these compounds.

3.4. NMR spectroscopy

The assignments of proton and carbon chemical shifts were made by a combined use of one- (^{1}H and APT) and two-dimensional (gCOSY, gHSQC and gHMBC) NMR spectra. Carbon and

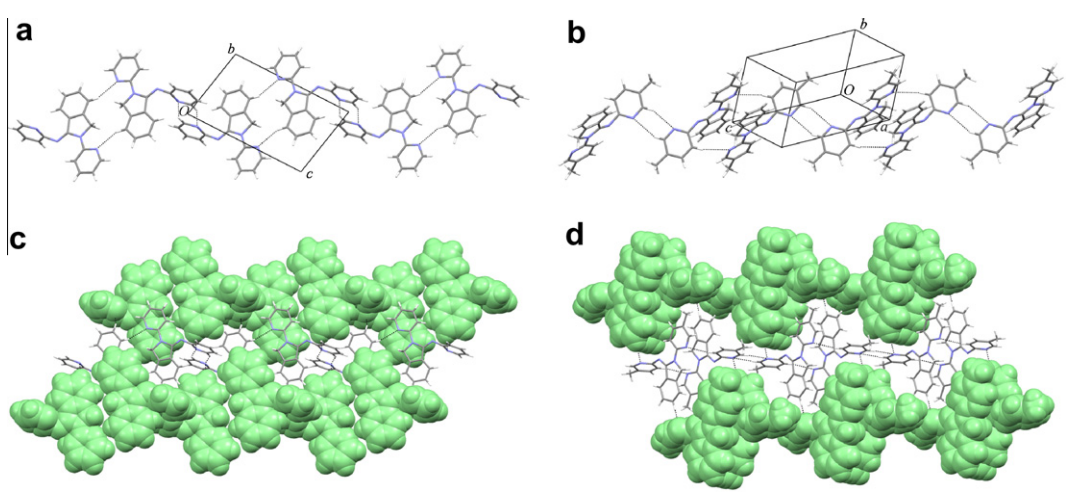

Fig. 3. Hydrogen bonding between molecules in the crystal structures of **8** and **9**: (a) chains of molecules in the structure of **8** viewed along the *b* axis, (b) chains of molecules in the structure of **9** viewed approximately along the 111 direction, (c) interconnection of chains into 2D-networks in the structure of **8**, and (d) interconnection of chains into 2D-networks in the structure of **9**.

Table 2
Geometry of intermolecular C–H···N contacts in compounds **8** and **9**.

Contact	d(C···N) (Å)	θ(C–H···N) (Å)	Symmetry operator
8			
C13–H13···N3	2.663	145.6	$2-x, -y, -z$
C6–H6···N4	2.672	155.0	$1-x, -y, -z$
C5–H5···N3	2.707	137.8	$x-1, y, z$
9			
C13–H13···N3	2.692	153.5	$-x, 1-y, -z$
C10–H10···N4	2.670	159.6	$-x, 2-y, -z$
C5–H5···N3	2.707	146.8	$x, 1+y, z$

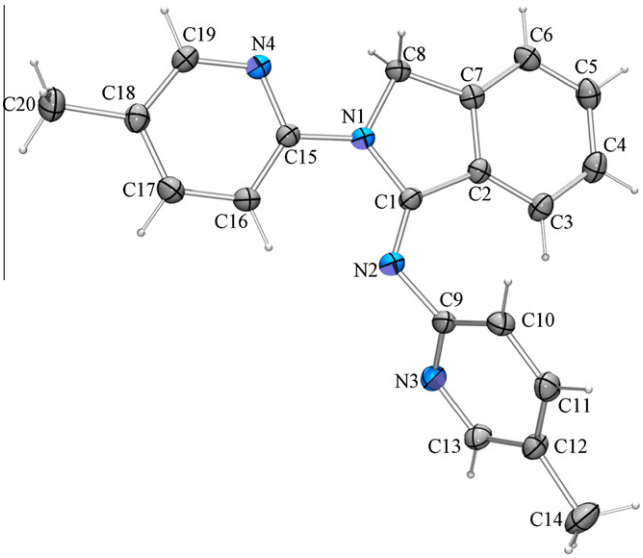

Fig. 4. Molecular structure of **9** with the atom labeling scheme. Thermal ellipsoids are drawn at the 50% probability level and hydrogen atoms are presented as spheres of arbitrary small radii.

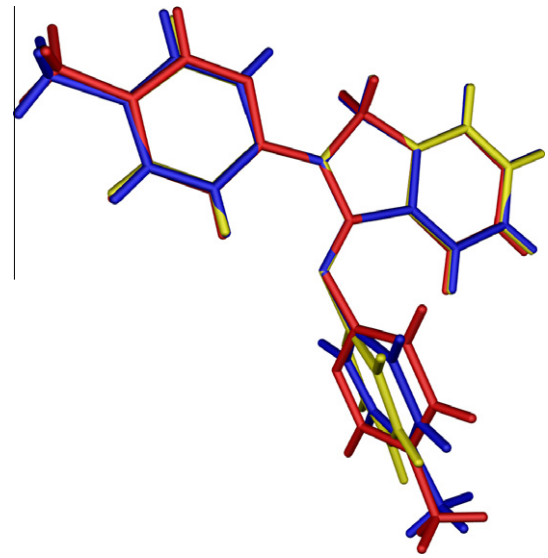

Fig. 5. Overlap of the molecules of **7** (blue), **8** (yellow) and **9** (red). The isoindoline system is taken to be in the same position in all three molecules. (For interpretation of the references to colour in this figure legend, the reader is referred to the web version of this article.)

Table 3
Melting points, enthalpies and entropies of fusion for compounds **8** and **9**.

	8	**9**
T/K	476.6	460.6
$\Delta_{fus}H$/kJ mol^{-1}	32.1	36.4
$\Delta_{fus}S$/J K^{-1} mol^{-1}	67.3	78.9

proton chemical shifts of compounds **6**–**9** are given in Table 4. The analysis of the recorded spectra did not show evidence of intramolecular hydrogen bonds in solution as found in the solid state.

Since the compounds **6**–**9** showed interesting biological activity we were also interested in their solution state structures. In order to check if conformation changes in solution compared to solid state we have performed NOESY experiments and analyzed all NOE cross peaks. Most of the NOE connectivities were in accordance with the solid state structures. Apart from the trivial NOE contacts some very interesting ones were also observed. The NOE analysis has shown that structures of compounds **6** and **7** are practically identical in DMSO solution. The same holds for **8** and **9**. However, some NOE cross peaks such as H3–H18,22 observed for **6** and **7** strongly suggested that these compounds adopted somewhat different conformation in solution compared to the one observed in the solid state (Fig. 5.).

The distance between protons H3 and H18 and H22 is approximately 5.5 Å in the solid state while in solution these protons must be much closer to account for the observed NOE cross peak in the NOESY spectrum. Furthermore, conformational differences between compounds having pyridine ring instead of benzene ring have also been detected. This primarily refers to the position of the pyridine ring attached to the imino group with respect to isoindoline system. Namely, in compounds **8** and **9** NOE contacts such as H8–H22 and H8–H21 have been detected which pointed towards close proximity of those moieties, as also observed in the solid state. However, similar contacts were not found for **6** and **7** where only the trivial H8–H9 cross peak was present in the spectrum. X-ray analysis have also shown some differences in the position of pyridine and benzene rings (Fig. 5.) but those were not as pronounced as in solution.

3.5. UV/Vis spectroscopic analysis

Measurements of the UV/Vis spectra of compounds **6**–**9** were undertaken in order to study their spectroscopic properties. Spectra can be visualized in Fig. 7 and all the results are summarized in Table 5.

Phenyl derivatives of isoindoline **6** and **7** showed one lower absorption maximum at 284 and 288 nm respectively and two strong absorption maxima, one at 237 and 239 nm respectively and both of them one at 210 nm. Pyridine derivatives of isoindoline **8** and **9** showed three absorption bands of similar intensity at 306, 231 and 209 nm and 312, 234 and 209 nm respectively. Pyridine derivatives **8** and **9** in comparison with phenyl derivatives **6** and **7** showed hypochromic shift of absorption maxima at lower wavelengths (at 231 and 234 nm respectively and at 209 nm both) and bathochromic shift for ~23 nm as well as hyperchromic shift at higher wavelength. The substituent effects of the electron-donating methyl group at phenyl and pyridine rings (compounds **7** and **9**) affects their absorption spectra producing a negligible bathochromic shift for ~6 nm in both cases (see Table 6).

3.6. Antiproliferative activity

This study was aimed to screen the antiproliferative effects of four isoindoline derivatives **6**–**9** on human tumor cell lines, as well as on normal (diploid) human fibroblasts (control cell line) in order to find potential candidates for further pre-clinical evaluation. The

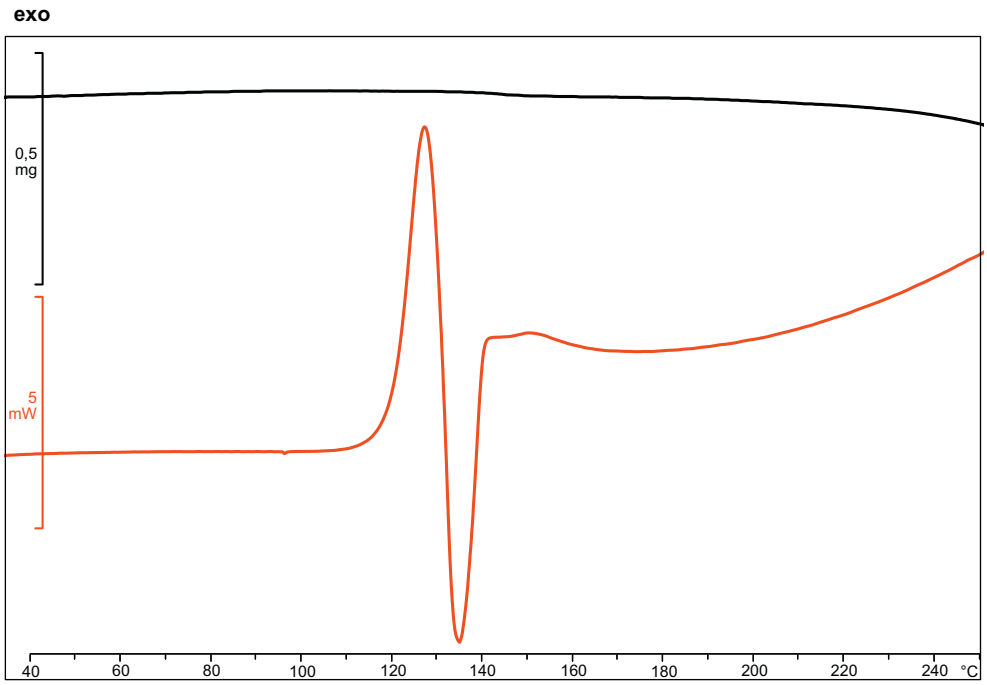

Fig. 6. The thermogravimetric and the DSC curve for **7**.

Table 4
Carbon and proton chemical shifts of compounds **6**–**9**.

Atom	**6**		**7**		**8**		**9**	
	^{1}H δ (ppm)	^{13}C δ (ppm)	^{1}H δ (ppm)	^{13}C δ (ppm)	^{1}H δ (ppm)	^{13}C δ (ppm)	^{1}H δ (ppm)	^{13}C δ (ppm)
1		152.670		152.729		153.677		154.174
2								
3	5.053	52.434	5.000	52.464	5.230	51.733	5.181	52.165
4		140.940		140.913		141.071		141.489
5	7.594	123.432	7.571	123.371	7.675	123.811	7.646	124.246
6	7.472	130.556	7.453	130.381	7.530	131.264	7.505	131.544
7	7.093	126.990	7.117		7.165	127.176	7.156	127.617
8	6.553	125.225	6.608	125.232	6.287	124.958	6.321	125.495
9		130.556		130.643		130.136		130.819
10		150.463		147.982		152.386		150.966
11	6.904	120.682	6.773	120.552				
12	7.323	129.137	7.117	129.612	8.453	147.728	8.267	147.903
13	7.093	122.025		130.526	7.134	118.542		127.799
14	7.323	129.137	7.117	129.612	7.846	137.681	7.657	138.584
15	6.904	120.682	6.773	120.552	8.825	114.015	8.709	114.022
16								
17		141.261		138.880		161.585		159.943
18	8.038	119.932	7.891	120.044				
19	7.394	128.525	7.190	128.922	8.369	148.665	8.184	148.861
20	7.093	122.781		131.726	7.147	118.621		127.617
21	7.394	128.525	7.190	128.922	7.786	138.132	7.590	139.160
22	8.038	119.932	7.891	120.044	7.002	115.871	6.884	115.831
23			2.318	20.463			2.289	17.719
24			2.288	20.358			2.320	17.872

in vitro screening on cell lines HeLa (cervical carcinoma), SW620 (colorectal adenocarcinoma, metastatic), MiaPaCa-2 (pancreatic carcinoma), MCF-7 (breast epithelial adenocarcinoma, metastatic), HepG2 (hepatocellular carcinoma) and WI38 (normal diploid human fibroblasts) was determined by standard procedure of the National Cancer Institute. A stronger growth inhibitory effect was observed only at the highest tested concentrations (1×10^{-4} M). The same cytotoxic effect was observed on the control fibroblasts WI38.

Phenyl substituted iminoisoindoline **6** showed only very weak antiproliferative activity on HepG2 cell line and was not active on other cell lines. *p*-Methylphenyl substituted compound **7** showed stronger non-specific antiproliferative effect on all tested cell lines as well as on the control fibroblasts WI38. Pyridine derivatives of 1-iminoisoinodoline **8** and **9** showed selective antiproliferative activity on HepG2 cell line, where unsubstituted pyridine derivative showed stronger activity.

4. Conclusion

In this work, we have presented the synthesis of novel 1-iminoisoindoline derivatives, their spectroscopic characterization, thermal analysis, structure determination in solid state and solution,

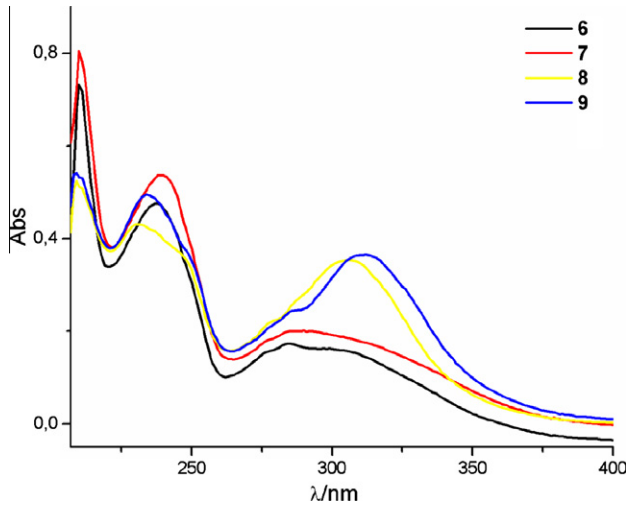

Fig. 7. Absorption spectra of **6–9** in ethanol at the concentration of 2.0×10^{-5} mol dm^{-3}.

Table 5
Electronic absorption data of **6–9** recorded in ethanol at the concentration of 2×10^{-5} mol dm^{-3}.

Compound	$\lambda_{abs,max}$ (nm)	$\varepsilon \times 10^3$ (dm^3 mol^{-1} cm^{-1})
6	284	8.7
	237	23.8
	210	36.5
7	288	10.1
	239	26.9
	210	40.3
8	306	17.7
	231	21.6
	209	26.0
9	312	18.3
	234	24.8
	209	27.0

Table 6
Inhibitory effects of compounds **6–9** on the growth of malignant tumor cell lines and normal human fibroblasts (WI 38).

IC_{50} (μM)[a]						
Compound	Cell lines					
	HeLa	MCF-7	HepG2	SW620	MiaPaCa-2	WI38
6	>100	>100	79.29	>100	>100	>100
7	59.97	88.14	46.81	45.12	56.80	58.13
8	>100	>100	42.91	85.35	>100	82.61
9	>100	95.14	79.88	>100	>100	>100

[a] IC_{50}; the concentration that causes a 50% reduction of the cell growth.

as well as their antiproliferative activity. Novel 1-iminoisoindoline derivatives were prepared from phthalaldehyde and corresponding amines in absolute ethanol. The presence of nitrogen in substituents on the isoindoline system was found to greatly increase the compounds' thermal stability. Structural analysis showed that conformations of the prepared compounds are not the same in solution and solid state. Prepared compounds were also tested on their antiproliferative activity *in vitro* on five human tumor cell lines as well as on normal (diploid) human fibroblasts. Those results are guidelines for further structural optimization studies.

Supplementary material

CCDC 799224–799226 contains the supplementary crystallographic data for this paper. These data can be obtained free of charge at www.ccdc.cam.ac.uk/conts/retrieving.html [or from the Cambridge Crystallographic Data Centre (CCDC), 12 Union Road, Cambridge CB2 1EZ, UK; fax:+44 (0)1223 336033; email: deposit@ccdc.cam.ac.uk].

Acknowledgements

The Ministry of Science, Education and Sport of the Republic of Croatia (Grant Nos. 125-0982464-1356, 119-1193079-3069, 335-0000000-3532 and 119-1191342-1083) supported this work.

References

[1] D. Berger, R. Citarella, M. Dutia, L. Greenberger, W. Hallett, R. Paul, D. Powell, J. Med. Chem. 42 (1999) 2145.
[2] L.A. Masterson, S.J. Croker, T.C. Jenkins, P.W. Howard, D.E. Thurston, Bioorg. Med. Chem. Lett. 14 (2004) 901.
[3] C. Shinji, S. Maeda, K. Imai, M. Yoshida, Y. Hashimoto, H. Miyachi, Bioorg. Med. Chem. 14 (2006) 7625.
[4] T.M. Percino, J.C. Basurto, K.S. Alavés Carbajal, N. Valle-Sandoval, J. Trujillo Ferrara, J. Mex. Chem. Soc. 53 (2009) 1.
[5] N. Gueven, J. Luff, C. Peng, K. Hosokawa, S.E. Bottle, M.F. Lavin, Free Radical Biol. Med. 41 (2006) 992.
[6] G.W. Muller, H.-W. Man, US Patent 7495,237 B2 2008.
[7] N.G. Kundu, M.W. Khan, R. Mukhopadhyay, J. Ind. Chem. Soc 78 (2001) 671.
[8] S. Van Goethem, P. Van, V. der Veken, A. Dubois, A.-M. Soroka, X. Lambeir, A. Chen, S. Haemers, I. Scharpe, K. De Meester, K. Augustyns, Bioorg. Med. Chem. Lett. 18 (2008) 4159.
[9] W.-T. Jiaang, J.-S. Chen, T. Hsu, S.-H. Wu, C.-H. Chien, C.-N. Chang, S.-P. Chang, S.-J. Lee, X. Chen, Bioorg. Med. Chem. Lett. 15 (2005) 687.
[10] J.-C. Souvie, C. Fugire, J.-P. Lecouve, US Patent 6320,058 B2 2001.
[11] E. Meggers, G.E. Atilla-Gokcumen, H. Bregman, J. Maksimoska, S.P. Mulcahy, N. Pagano, D.S. Williams, Synlett 8 (2007) 1177.
[12] J. Kaizer, B. Kripli, G. Speier, L. Parkanyi, Polyhedron 28 (2009) 933.
[13] M. Horiuchi, K. Ohnishi, N. Iwase, Y. Nakajima, K. Tounai, M. Yamashita, Y. Yamada, Biosci. Biotechnol. Biochem. 67 (2003) 1580.
[14] A. Pugin, K.E. Burdeska, A. Staub, US Patent 3484,454 1969.
[15] B. Lotsch, US Patent 4719,300 1988.
[16] Y. Mulyana, C.J. Kepert, L.F. Lindoy, J.C. McMurtie, Eur. J. Inorg. Chem (2005) 2470.
[17] J.M. Chitanda, D.E. Prokopchuk, J.W. Quail, S.R. Foley, Dalton Trans. (2008) 6023.
[18] J.M. Chitanda, J.W. Quail, S.R. Foley, J. Organomet. Chem. 694 (2009) 1542.
[19] M. Broering, C. Kleeberg, Inogr. Chim. Acta 362 (2009) 1065.
[20] E.V. Pankratova, G.N. Rodionova, B.E. Zaitsev, V.A. Titkov, Chem. Heterocycl. Comp. 13 (1977) 54.
[21] A. Cul, A. Daich, B. Decroix, G. Sanz, L. Van Hijfte, Tetrahedron 60 (2004) 11029.
[22] H. Yoshida, H. Fukushima, T. Morishita, J. Ohshita, A. Kunai, Tetrahedron 63 (2007) 4793.
[23] E.R. Bonfield, C.-J. Li, Adv. Synth. Catal. 350 (2008) 370.
[24] T. DoMinh, A.L. Johnson, J.E. Jones, P.P. Senise Jr, J. Org. Chem. 42 (1977) 4217.
[25] R. Grigg, H.Q.N. Gunaratne, V. Sridharan, Chem. Commun. (1985) 1183.
[26] S.M. Allin, C.C. Hodkinson, N. Taj, Synlett (1996) 781.
[27] I. Takahashi, T. Kawakami, E. Hirano, H. Yokota, H. Kitajima, Synlett (1996) 353.
[28] J.M. Chitanda, D.E. Prokopchuk, J.W. Quail, S.R. Foley, Organometallics 27 (2008) 2337.
[29] Oxford Diffraction, CrysAlis CCD and CrysAlis RED. Version 1.170. Oxford Diffraction Ltd., Wroclaw, Poland, 2003.
[30] G.M. Sheldrick, Acta Cryst. A64 (2008) 112.
[31] L.J. Farrugia, J. Appl. Cryst. 32 (1999) 837.
[32] *STARe Software V.9.01.*, MettlerToledo GmbH, 2006.
[33] I. Takahashi, K. Nishiuchi, R. Miyamoto, M. Hatanaka, H. Uchida, K. Isa, A. Sakushima, S. Hosoi, Lett. Org. Chem. 2 (2005) 40.
[34] L.-N. Zhu, S. Gao, L.H. Huo, H. Zhao, Acta Cryst. E63 (2007) o4111.
[35] M. Akkurt, S.O. Yildirim, S.S. Al-Shihry, O. Buyukgungor, Acta Cryst. E62 (2006) o2226.
[36] I. Takahashi, R. Miyamoto, K. Nishiuchi, M. Hatanaka, A. Yamano, A. Sakushima, S. Hosoi, Heterocycles 63 (2004) 1267.
[37] J.M. Chitanda, J.W. Quail, S.R. Foley, Acta Cryst. E64 (2008) m907.
[38] V. Stilinović, D. Cinčić, B. Kaitner, Acta Chim. Slov. 55 (2008) 874.